PHYSICAL REVIEW E VOLUME 59, NUMBER 3 MARCH 1999

Phase separation kinetics of liquid crystalline polymers: Effect of orientational order

Jun-ichi Fukuda
Department of Physics, Kyoto University, Kyoto 606-8502, Japan

(Received 21 September 1998)

Phase separation kinetics of main-chain liquid crystalline polymers (LCP's) is investigated by numerically solving time-dependent Ginzburg-Landau equations for the compositional order parameter ϕ and the orientational order parameter S_{ij}. The kinetic coefficients are evaluated by using the biased reptation model with a microscopic model of wormlike chains. In numerical simulations we find the formation of a percolated network structure rich in LCP's that resembles that observed in experiments. In our kinetic equations the coupling between compositional order and orientational order appears in (i) the presence of the off-diagonal kinetic coefficient $\Lambda_{\phi S}$ and (ii) the dependence of the kinetic coefficients on S_{ij} (LCP's tend to diffuse parallel to the nematic orientation). We show by a linear analysis of the growing modes that the presence of $\Lambda_{\phi S}$ suppresses the growth of the compositional order in the early stage. We also show that the tendency of LCP's to diffuse parallel to the nematic orientation is responsible for the breakage of the network structure.
[S1063-651X(99)14303-4]

PACS number(s): 61.25.Hq, 64.70.Md, 64.75.+g

I. INTRODUCTION

The kinetics of phase separation has been an important and challenging problem in statistical physics [1] and polymeric systems have attracted great theoretical and technological interest. Experimental studies of phase separation kinetics in polymeric systems have thus been extensively performed [2] and it has been shown that binary homopolymer blends belong to the universality class of simple fluids in many cases, although the temporal and spatial scales are much more enlarged than in simple fluids. However, phase separation in polymeric systems can be significantly different in dynamical as well as static aspects from that in simple fluids because polymer chains have internal degrees of freedom due to the chain connectivity and are spatially extended because of their large molecular size [3–5]. For example, block copolymers, composed of different types of homopolymer chains covalently connected to one another, show microphase separation to form rich variety of periodic structures such as lamellae, cylinders, and spheres depending on the temperature and the composition of a single chain. Macrophase separation does not occur in block copolymer melts because the characteristic size of phase-separated domains cannot exceed the length of a single polymer chain. Recent studies on kinetics of block copolymer melts [6,7] have shown that changes in the chain conformation at the interfaces between phase-separated domains have an important effect on the phase transition kinetics. It has also been shown that the dynamical aspect of phase separation in polymer solutions is significantly different from that of simple liquids. By quenching semidilute polymer solutions into an unstable temperature region, a transient network structure rich in polymers has been observed [8]. This unusual behavior is attributed to the large difference in viscoelastic properties between polymers and solvents [8–11].

Liquid crystalline polymers (LCP's), which have attracted much technological attention because of their industrial applications such as optical devices and fibers of high tensile strength, are another good example whose phase separation is significantly different from that of simple liquids. Main-chain LCP's have mesogenic units in their backbones and show nematic order in suitable conditions. From statistical mechanical point of view, phase separation of LCP's is a fascinating but difficult subject because of the coupling between the compositional order and the orientational order. Phase diagram of systems containing LCP's is quite complex and sensitively depends on the properties of the system such as isotropic and anisotropic interaction parameters [12]. Experiments have been performed concerning the phase separation kinetics and morphology of LCP's. For example, phase separation of LCP solutions lead to fibrillar network domains rich in LCP's even when the volume fraction of LCP's is relatively small [13]. Mixtures of LCP's and low-molecular-weight liquid crystals in a nematic state exhibit a nematic-nematic phase separation to form anisotropic droplets [14] or striated patterns parallel to the nematic direction [15], which clearly indicates that orientational order has a significant effect on compositional phase separation. LCP's also have an experimental advantage that we can pursue a real space analysis on mechanism of phase separation because the isotropic phase poor in LCP's and the anisotropic phase rich in LCP's give a remarkable contrast by polarized light microscopy [16,17]. Observation of a process of phase separation in 50:50 mixtures of LCP's and flexible polymers shows that percolated network structures rich in LCP's are initially formed and that they break up and shrink to droplets [16,17].

The aim of this article is to investigate phase separation kinetics of LCP's. As noted in the preceding paragraph, orientational order as well as compositional order must be traced to describe the process of phase separation and the coupling of these two order parameters makes the problem quite complicated. Hence there have not been enough theoretical studies focused on the dynamical aspect of the phase separation in LCP's, and it still remains unclear how orientational order affects the phase separation kinetics of LCP's in late stages. Some previous attempts were based on purely phenomenological arguments and by using the time depen-

1063-651X/99/59(3)/3275(14)/$15.00

dent Ginzburg-Landau (TDGL) equations for the order parameters, linear analysis of the growing mode [18], and numerical analysis of the time evolution of domain morphology [19] were given. There also exist some other studies on a microscopic basis. They are based on the Doi equation [20], the equation for time evolution of the positional and orientational distribution function for rigid rods. Shimada, Doi, and Okano [21] derived the linearized equations describing the growth of the order parameters by projecting the Doi equation to the equations for the compositional and the orientational order parameters. Liu and Fredrickson [22] derived the TDGL equations and the kinetic coefficients were derived by using the Doi equation and a dynamical random phase approximation. In this work we will consider the TDGL equations of motion for the compositional scalar order parameter ϕ and the orientational order parameter of second-rank tensor S_{ij}, and derive the kinetic coefficients on a different basis, the biased reptation model [6]. Characteristic of our model are the presence of the off-diagonal kinetic coefficient $\Lambda_{\phi S}$ and the introduction of anisotropic diffusion induced by orientational order. Liu and Fredrickson [22] have already shown that the off-diagonal kinetic coefficient should appear in the kinetic equations. However, phenomenological analyses [18,19] have neglected this off-diagonal kinetic coefficient and our numerical studies [23,24] have shown that it has a significant effect on phase separation kinetics. Anisotropic diffusion naturally arises in a nematic state because LCP's tend to make Brownian motion parallel to themselves rather than perpendicular to themselves in nondilute solutions [20]. However, so far as we know, there has been no attempt, even phenomenologically, to incorporate this kind of anisotropy to kinetic coefficients to reproduce anisotropic diffusion.

This article is organized as follows: In Sec. II, we formulate our model. We define the compositional and the orientational order parameters in Sec. II A. In Sec. II B, we give the Hamiltonian of a single chain that will be used throughout the calculations given below. In Sec. II C, we show the free energy functional of the system in terms of the order parameters defined in Sec. II A. Derivation of the kinetic equations is given in Sec. II D. In Sec. III, we give the results of the numerical integration of our model. In Sec. IV, we perform a linear analysis of the growing modes from an isotropic and homogeneous state. we give a brief conclusion in Sec. V.

II. MODEL

A. Order parameters

We consider a solution of main-chain liquid crystalline homopolymers. As noted in the Introduction, the orientational order as well as the compositional order (or the density of the polymers) must be specified to describe the state of the system. To this end we introduce the following two order parameters. One is the volume fraction of the polymers defined as

$$\phi(\boldsymbol{r})=\sum_{\alpha}\int_0^L d\tau\,\hat{\phi}^{\alpha}(\tau,\boldsymbol{r}) \tag{1}$$

with

$$\hat{\phi}^{\alpha}(\tau,\boldsymbol{r})=\frac{v_0}{b}\,\delta(r-\boldsymbol{R}^{\alpha}(\tau)). \tag{2}$$

Here v_0 and b are the monomer volume and the average distance between adjacent monomers, respectively, and $L=Nb$, N being the degree of polymerization. The α is the chain index and the configuration of the α-th chain is represented by $\boldsymbol{R}^{\alpha}(\tau)$, where τ parametrizes the position along the chain running from 0 to L. The other is the orientational order, which is defined by

$$S_{ij}(\boldsymbol{r})=\sum_{\alpha}\int_0^L d\tau\,\hat{S}_{ij}^{\alpha}(\tau,\boldsymbol{r}) \tag{3}$$

with

$$\hat{S}_{ij}^{\alpha}(\tau,\boldsymbol{r})=\frac{v_0}{b}\left[u_i^{\alpha}(\tau)u_j^{\alpha}(\tau)-\frac{1}{d}\delta_{ij}\right]\delta(r-\boldsymbol{R}^{\alpha}(\tau)), \tag{4}$$

where

$$u_i^{\alpha}(\tau)\equiv\frac{\partial R_i^{\alpha}(\tau)}{\partial\tau} \tag{5}$$

and d is the spatial dimension of the system. From the definition S_{ij} is symmetric and $S_{ij}=0$ in the equilibrium isotropic state.

B. Single-chain Hamiltonian

In the calculation of the free energy [25] and the kinetic coefficients given below, a microscopic model for a single chain is necessary. A main-chain LCP is stiff due to the mesogenic units along the chain and the bending energy of a chain can be described as

$$\beta\mathcal{H}_{bend}=\int_0^L d\tau\frac{\epsilon b}{2}\left(\frac{\partial\boldsymbol{u}(\tau)}{\partial\tau}\right)^2, \tag{6}$$

where β and ϵ are the inverse temperature and the (dimensionless) bending elastic constant, respectively, and $\boldsymbol{u}$ is defined in Eq. (5). Equation (6) with the constraint of local inextensibility $|\boldsymbol{u}(\tau)|=1$ is a typical model of a wormlike chain and the properties of this model have been extensively studied [26–28].

Another model has also been studied for a wormlike chain where local inextensibility of the chain is not imposed [28–31]. Then for the model to be well defined, a penalty for the stretching of the chain must be added to the Hamiltonian and the resulting energy for a single chain can be written as

$$\beta\mathcal{H}_0=\int_0^L d\tau\left\{\frac{d}{2lb}\boldsymbol{u}(\tau)^2+\frac{\epsilon b}{2}\left(\frac{\partial\boldsymbol{u}(\tau)}{\partial\tau}\right)^2\right\}, \tag{7}$$

where the first term penalizes the stretching of the chain and another elastic constant l is introduced. Here we impose the constraint $1=\langle\boldsymbol{u}(\tau)^2\rangle_0\equiv\int\mathcal{D}\boldsymbol{R}u(\tau)^2\exp(-\beta\mathcal{H}_0)/\int\mathcal{D}\boldsymbol{R}\exp(-\beta\mathcal{H}_0)$ instead of the constraint of local inextensibility $|\boldsymbol{u}(\tau)|=1$. Then we obtain [25,31]

$$l=\frac{4\epsilon}{d} \tag{8}$$

and the properties of a single chain can be described by a single bending elastic constant ϵ.

In our calculation of the free energy [25], Eq. (7) has been adopted as a single chain Hamiltonian instead of Eq. (6) with the constraint of local inextensibility because the Gaussian property of the Hamiltonian (7) greatly facilitates the calculation of the free-energy functional. Therefore we also adopt Eq. (7) for the calculation of the kinetic coefficients given below. We note that since the model given by Eq. (6) allows the fluctuation of $|\boldsymbol{u}(\tau)|$, the orientational order parameter S_{ij} is not necessarily traceless, although it is traceless in the usual liquid crystals [32]. We also note that Gupta and Edwards [34] have extensively studied the phase behavior of LCP's using the Hamiltonian (7).

Finally, for the sake of convenience in the discussion below, we introduce the fields $h_\phi(\boldsymbol{r})$ and $h_{S_{ij}}(\boldsymbol{r})$ conjugate to the order parameters $\phi(\boldsymbol{r})$ and $S_{ij}(\boldsymbol{r})$, respectively. The Hamiltonian due to these conjugate fields can be written as

$$\beta\mathcal{H}_1=\int d\boldsymbol{r}\int_0^L d\tau\{h_\phi(\boldsymbol{r})\hat{\phi}(\tau,\boldsymbol{r})+h_{S_{ij}}(\boldsymbol{r})\hat{S}_{ij}(\tau,\boldsymbol{r})\}, \tag{9}$$

where $\hat{\phi}(\tau,\boldsymbol{r})$ and $\hat{S}_{ij}(\tau,\boldsymbol{r})$ have been defined in Eqs. (2) and (4). Hereafter summations over repeated indices are implied. The total Hamiltonian for a single chain is

$$\beta\mathcal{H}_{tot}=\beta(\mathcal{H}_0+\mathcal{H}_1). \tag{10}$$

C. Free energy

In this subsection, we briefly review the calculation of the free-energy functional in terms of the order parameters ϕ and S_{ij} [25]. There have been numerous studies concerning the phase diagram of systems containing LCP's and Liu and Fredrickson derived the free-energy functional for semiflexible polymer blends as a Landau-de Gennes expansion in terms of the orientational tensorial order parameter [33]. Our calculation of the free-energy functional is similar to that of Liu and Fredrickson except that our calculation uses the single-chain Hamiltonian (7) while that of Liu and Fredrickson is based on the microscopic model of an inextensible wormlike chain (6). In the mean field approximation, the form of the free-energy functional is [25]

$$\beta F\{\phi,S_{ij}\}=-\int d\boldsymbol{r}\left(\frac{1}{v_0N}\phi(\boldsymbol{r})+h_\phi(\boldsymbol{r})\phi(\boldsymbol{r}) + h_{S_{ij}}(\boldsymbol{r})S_{ij}(\boldsymbol{r})\right). \tag{11}$$

The relation between order parameters and conjugate fields for noninteracting ideal chains is given by

$$\phi(\boldsymbol{r})=-\frac{\delta z_0\{h_\phi,h_{S_{ij}}\}}{\delta h_\phi(\boldsymbol{r})}, \tag{12}$$

$$S_{ij}(\boldsymbol{r})=-\frac{\delta z_0\{h_\phi,h_{S_{ij}}\}}{\delta h_{S_{ij}}(\boldsymbol{r})}, \tag{13}$$

where $z_{-0}\{h_\phi,h_{S_{ij}}\}$ is the partition function of a single chain,

$$\begin{aligned}z_{-0}\{h_\phi,h_{S_{ij}}\}&=\tilde{\mathcal{Z}}\int \mathcal{D}\boldsymbol{R}(\tau)\exp(-\beta\mathcal{H}_{tot})\\&=\mathcal{Z}\langle\exp(-\beta\mathcal{H}_1)\rangle_0.\end{aligned} \tag{14}$$

Here $\tilde{\mathcal{Z}}$ is the contribution from the kinetic energy and $\mathcal{Z}=\tilde{\mathcal{Z}}\int\mathcal{D}\boldsymbol{R}(\tau)\exp(-\beta\mathcal{H}_0)$. The average in (14) is taken over the unperturbed Hamiltonian and defined by

$$\langle\cdots\rangle_0=\int\mathcal{D}\boldsymbol{R}(\tau)\cdots\exp(-\beta\mathcal{H}_0)/\int\mathcal{D}\boldsymbol{R}(\tau)\exp(-\beta\mathcal{H}_0). \tag{15}$$

Monomer interaction is taken into account by the random phase approximation (RPA). In the RPA, response of polymers to the fields h_ϕ and $h_{S_{ij}}$ is considered to be the same as that of noninteracting polymers, that is, the relation between the order parameters ϕ and S_{ij} and the conjugate fields h_ϕ and $h_{S_{ij}}$ for interacting chains is also given by Eqs. (12) and (13). However, the fields h_ϕ and $h_{S_{ij}}$ themselves are corrected to take into account monomer interactions as

$$h_\phi(\boldsymbol{r})=h^0_\phi(\boldsymbol{r})+h^{int}_\phi(\boldsymbol{r}), \tag{16}$$

$$h_{S_{ij}}(\boldsymbol{r})=h^0_{S_{ij}}(\boldsymbol{r})+h^{int}_{S_{ij}}(\boldsymbol{r}), \tag{17}$$

where h^0_ϕ and $h^0_{S_{ij}}$ are the fields that noninteracting polymers feel and their explicit form, which will be discussed below, can be obtained by inverting Eqs. (12) and (13). The additional fields h^{int}_ϕ and $h^{int}_{S_{ij}}$ represent monomer interaction. The isotropic interaction that favors demixing is in h^{int}_ϕ and the anisotropic interaction that induces nematic ordering and the penalty for the fluctuation of segment length can be incorporated in $h^{int}_{S_{ij}}$. The explicit form of h^{int}_ϕ and $h^{int}_{S_{ij}}$ are given when we discuss the final form of the free-energy functional.

The calculation of h^0_ϕ and $h^0_{S_{ij}}$ requires the evaluation of $z_{-0.}$ However, we cannot calculate z_{-0} analytically and we make a perturbation expansion in terms of $h^0_{S_{ij}}$ and a gradient expansion. Fortunately in zeroth order in the gradients and for the rigid rod limit ($\epsilon\rightarrow\infty$), we can evaluate z_{-0} exactly and inversion of Eqs. (12) and (13) yields

$$\begin{aligned}v_0Nh^0_\phi=&-\ln\left(\frac{\phi}{v_0N\mathcal{Z}}\right)-\tfrac{1}{2}\mathrm{Tr}\ln(\mathsf{1}+d\mathsf{Q})\\&-\tfrac{1}{2}(\mathsf{1}+d\mathsf{Q})^{-1}_{ij}dQ_{ji},\end{aligned} \tag{18}$$

$$-\frac{v_0N}{d}(h^0_{S_{ij}}+h^0_{S_{ji}})=(\mathsf{1}+d\mathsf{Q})^{-1}_{ik}dQ_{kj}, \tag{19}$$

where

$$Q_{ij}(\boldsymbol{r})\equiv\frac{S_{ij}(\boldsymbol{r})}{\phi(\boldsymbol{r})} \tag{20}$$

is the orientational order per segment, $\mathsf{1}$ is a $d\times d$ unit matrix and $(\mathsf{1}+d\mathsf{Q})^{-1}_{ij}$ is the element of the inverse matrix of $\mathsf{1}+d\mathsf{Q}$. Tr implies taking the trace of a matrix.

In Ref. [25], the gradient expansion up to second order is taken in evaluating z_{-0} and only the terms up to second order in Q_{ij} are retained for the second-order terms in the gradients. Taking into account the interaction terms and the degrees of freedom of the solvents, we obtain the final form of the free energy as

$$
\begin{aligned}
F=\frac{1}{v_0\beta}\int d\mathbf{r}\Bigg\{&\frac{\phi}{N}\ln\phi+\frac{1-\phi}{N'}\ln(1-\phi)+\chi\phi(1-\phi)\\
&-\frac{\phi}{2N}\mathrm{Tr}\{\ln(1+d\mathsf{Q})-d\mathsf{Q}\}-\frac{1}{2}w\phi^2\mathrm{Tr}(\mathsf{Q}-(1/d)\mathrm{Tr}\,\mathsf{Q})^2\\
&+\tfrac{1}{2}W\phi(\mathrm{Tr}\,\mathsf{Q})^2+\frac{1}{2\phi}C_0(\partial_i\phi)^2\\
&+L_0\left(\partial_i\phi\partial_jQ_{ij}+\frac{1}{2\phi}Q_{ij}\partial_i\phi\partial_j\phi\right)+\tfrac{1}{2}L_1\phi(\partial_kQ_{ij})^2\\
&+\tfrac{1}{2}L_2[\tfrac{1}{2}(\phi\partial_iQ_{ij}\partial_kQ_{kj}+\phi\partial_kQ_{ij}\partial_iQ_{jk})]\Bigg\}. \qquad (21)
\end{aligned}
$$

The first line is the conventional Flory-Huggins energy with an isotropic interaction parameter χ and $N'=1$. When we consider the blends of LCP's and another kind of flexible polymers, N' is the degree of the polymerization of the flexible polymers. The second line is the configurational entropy due to orientational order. The first term in the third line is the Maier-Saupe anisotropic interaction [32] that favors nematic order and the second term in the third line is added as a penalty for the fluctuation of the segment length. The last two lines are the gradient energy with $C_0=Nb^2/12d$, $L_0=Nb^2/12$, $L_1=dNb^2/24$ and $L_2=dNb^2/6$ [25]. The terms proportional to L_1 and to L_2 are the Frank elastic energy. We note that the free energy of an interface parallel to the nematic orientation is lower than a perpendicular one due to the terms proportional to L_0.

The phase behavior is quite complicated and sensitively depends on the temperature dependence of the interaction parameters χ and w. In a two-dimensional system $(d=2)$ where simulations discussed below are carried out, second-order isotropic-nematic (I-N) transition occurs at $wN\phi=2$, in contrast to the first-order I-N transition at $wN\phi=4.051\,41$ in a three-dimensional system [25]. When χ is large enough, compositional phase separation can lead to an LCP-rich phase with $wN\phi>2$ and an LCP-poor phase with $wN\phi<2$. In this situation, phase separation occurs into an LCP-rich nematic phase and an LCP-poor isotropic phase. Phase separation of this type is expected in a deep quench and is considered in the simulations given below.

D. Kinetic equations

1. Biased reptation model

In this subsection, we will derive the equations of motion for the order parameters ϕ and S_{ij}. So far as we know, there has been only one theoretical study where the equations of motion for the compositional and the orientational order parameters are derived on a microscopic basis. Liu and Fredrickson [22] considered a mixture of rigid rods and flexible coils and derived the equations of motion for the order parameters using a dynamical random phase approximation and the Doi equation [20], the equation of motion for the positional and orientational distribution function of rigid rods. Our derivation of the equations of motion is on a different basis, the biased reptation model [6]. In the biased reptation model, polymer chains make the Brownian motion under the fields they feel (h_ϕ and $h_{S_{ij}}$ in our case). A crucial assumption of this model is that polymer chains can move only along themselves because of the topological constraints imposed by the surrounding chains. That is, only the translational diffusion parallel to the chains is allowed and we neglect the rotational diffusion and the translational diffusion perpendicular to the chain, which are suppressed in nondilute solutions due to the entanglement [20]. We also neglect the hydrodynamic effect, though it might play an important role in late stage phase separation.

Here we briefly review the argument of the biased reptation model by Kawasaki and Sekimoto [6] and show how their argument can be extended to our case. The reptation motion of a single chain along itself can be represented by a single parameter $x(t)$, which has the same unit as the parameter τ characterizing the position of the segment along the chain. The Langevin equation for x can be given by

$$\frac{dx}{dt}=-D_c\beta\frac{d\mathcal{H}_{tot}(x)}{dx}+\zeta_x. \qquad (22)$$

Here D_c is the diffusion constant of motion along the chain and ζ_x is a thermal noise satisfying the fluctuation-dissipation theorem. The single-chain Hamiltonian $\mathcal{H}_{tot}$ is given in Sec. II B and can be considered here as a function of x. Using Eq. (9), we obtain after some manipulation

$$
\begin{aligned}
\beta\frac{d\mathcal{H}_{tot}(x)}{dx}=\int d\mathbf{r}\int_0^L d\tau\Bigg\{&h_\phi(\tau,\mathbf{r})\frac{\partial}{\partial\tau}\hat{\phi}(\tau,\mathbf{r})\\
&+h_{S_{ij}}(\tau,\mathbf{r})\frac{\partial}{\partial\tau}\hat{S}_{ij}(\tau,\mathbf{r})\Bigg\}. \qquad (23)
\end{aligned}
$$

Here we assume that h_ϕ and $h_{S_{ij}}$ are a function of τ and $\mathbf{r}$. Noticing that $A(\tau,t+dt)=A(\tau+dx,t)$, A being an arbitrary function of τ, we can derive the following identities:

$$\frac{\partial}{\partial t}\hat{\phi}(\tau,\mathbf{r})=\frac{dx}{dt}\frac{\partial}{\partial\tau}\hat{\phi}(\tau,\mathbf{r}), \qquad (24)$$

$$\frac{\partial}{\partial t}\hat{S}_{ij}(\tau,\mathbf{r})=\frac{dx}{dt}\frac{\partial}{\partial\tau}\hat{S}_{ij}(\tau,\mathbf{r}). \qquad (25)$$

Equations (1), (3), (22), (23), (24), and (25) yield

$$
\begin{aligned}
\frac{\partial}{\partial t}\phi(\mathbf{r})=-D_cn\int d\mathbf{r}'\int_0^L d\tau\int_0^L d\tau'\Bigg\{&h_\phi(\tau',\mathbf{r}')\frac{\partial^2}{\partial\tau\partial\tau'}\\
&\times\langle\hat{\phi}(\tau,\mathbf{r})\hat{\phi}(\tau',\mathbf{r}')\rangle\\
&+h_{S_{ij}}(\tau',\mathbf{r}')\frac{\partial^2}{\partial\tau\partial\tau'}\langle\hat{\phi}(\tau,\mathbf{r})\hat{S}_{ij}(\tau',\mathbf{r}')\rangle\Bigg\}+\xi_\phi,
\end{aligned}
\qquad (26)
$$

$$\frac{\partial}{\partial t}S_{ij}(\mathbf{r})=-D_c n\int d\mathbf{r}'\int_0^L d\tau\int_0^L d\tau'\Biggl\{h_\phi(\tau',\mathbf{r}')\frac{\partial^2}{\partial\tau\partial\tau'}\times\langle\hat{S}_{ij}(\tau,\mathbf{r})\hat{\phi}(\tau',\mathbf{r}')\rangle+h_{S_{kl}}(\tau',\mathbf{r}')\frac{\partial^2}{\partial\tau\partial\tau'}\times\langle\hat{S}_{ij}(\tau,\mathbf{r})\hat{S}_{kl}(\tau',\mathbf{r}')\rangle\Biggr\}+\xi_{S_{ij}},\tag{27}$$

where n is the number of polymer chains in the system and ξ_ϕ and $\xi_{S_{ij}}$ are the Gaussian noise terms. We have made a local equilibrium assumption and the average in Eq. (33) should be taken for the local equilibrium state specified by $\{\phi(\mathbf{r}),S_{ij}(\mathbf{r})\}$. Equation (23) can be interpreted as

$$\beta\delta\mathcal{H}_{tot}=\int d\mathbf{r}\int_0^L d\tau\{h_\phi(\tau,\mathbf{r})\,\delta\hat{\phi}(\tau,\mathbf{r})+h_{S_{ij}}(\tau,\mathbf{r})\,\delta\hat{S}_{ij}(\tau,\mathbf{r})\},\tag{28}$$

and we get

$$\beta\frac{\delta\mathcal{H}_{tot}}{\delta\psi(\tau,\mathbf{r})}=h_\psi(\tau,\mathbf{r}),\quad(\psi=\phi\ \text{or}\ S_{ij}).\tag{29}$$

When we extrapolate this result to the case where $\mathcal{H}_{tot}$ is replaced by the free energy of the entire system F and $\delta\psi(\tau,\mathbf{r})$ by the order parameter variation occurring in the many chain system, we can take [6]

$$h_\psi(\tau,\mathbf{r})\rightarrow\frac{\delta(\beta F)}{\delta\psi(\mathbf{r})}(\psi=\phi\ \text{or}\ S_{ij}),\tag{30}$$

and we obtain the final expression for the equations of motion for the order parameters as

$$\frac{\partial}{\partial t}\phi(\mathbf{r})=\int d\mathbf{r}'\Biggl\{\Lambda_{\phi\phi}(\mathbf{r},\mathbf{r}')\frac{\delta(\beta F)}{\delta\phi(\mathbf{r}')}+\Lambda_{\phi S_{kl}}(\mathbf{r},\mathbf{r}')\frac{\delta(\beta F)}{\delta S_{kl}(\mathbf{r}')}\Biggr\}+\xi_\phi,\tag{31}$$

$$\frac{\partial}{\partial t}S_{ij}(\mathbf{r})=\int d\mathbf{r}'\Biggl\{\Lambda_{\phi S_{ij}}(\mathbf{r}',\mathbf{r})\frac{\delta(\beta F)}{\delta\phi(\mathbf{r}')}+\Lambda_{S_{ij}S_{kl}}(\mathbf{r},\mathbf{r}')\frac{\delta(\beta F)}{\delta S_{kl}(\mathbf{r}')}\Biggr\}+\xi_{S_{ij}},\tag{32}$$

with the kinetic coefficients

$$\Lambda_{\psi_1\psi_2}(\mathbf{r},\mathbf{r}')=-D_c n\int_0^L d\tau\int_0^L d\tau'\frac{\partial^2}{\partial\tau\partial\tau'}\times\langle\hat{\psi}_1(\tau,\mathbf{r})\hat{\psi}_2(\tau',\mathbf{r}')\rangle,\quad(\psi_1,\psi_2=\phi\ \text{or}\ S_{ij}).\tag{33}$$

The Gaussian noise terms ξ_ϕ and $\xi_{S_{ij}}$ satisfy the fluctuation-dissipation relation

$$\langle\xi_{\psi_1}(\mathbf{r},t)\xi_{\psi_2}(\mathbf{r}',t')\rangle=-2\Lambda_{\psi_1\psi_2}(\mathbf{r},\mathbf{r}')\,\delta(t-t'),\quad(\psi_1,\psi_2=\phi\ \text{or}\ S_{ij}).\tag{34}$$

2. Calculation of the kinetic coefficients

The final task to obtain the equations of motion for the order parameters is to evaluate the kinetic coefficients given by Eq. (33). As can be seen from Eq. (33), the kinetic coefficients are determined by the conformation of a single chain in a local equilibrium state specified by $\{\phi(\mathbf{r}),S_{ij}(\mathbf{r})\}$ and the average in Eq. (33) can be taken by using the full Hamiltonian of a single chain as

$$\langle\hat{\psi}_1(\tau,\mathbf{r})\hat{\psi}_2(\tau',\mathbf{r}')\rangle=\frac{\int\mathcal{D}\mathbf{R}\,\hat{\psi}_1(\tau,\mathbf{r})\,\hat{\psi}_2(\tau',\mathbf{r}')\exp(-\beta\mathcal{H}_{tot})}{\int\mathcal{D}\mathbf{R}\exp(-\beta\mathcal{H}_{tot})}=\frac{\langle\hat{\psi}_1(\tau,\mathbf{r})\,\hat{\psi}_2(\tau',\mathbf{r}')\exp(-\beta\mathcal{H}_1)\rangle_0}{\langle\exp(-\beta\mathcal{H}_1)\rangle_0}.\tag{35}$$

The average over an unperturbed Hamiltonian $\langle\cdots\rangle_0$ is defined in Eq. (15). The conjugate fields $h_\phi(\mathbf{r})$ and $h_{S_{ij}}(\mathbf{r})$ in $\mathcal{H}_1$ should be taken self-consistently so that the local equilibrium state $\{\phi(\mathbf{r}),S_{ij}(\mathbf{r})\}$ is realized. Unfortunately, rigorous evaluation of the average appearing in Eq. (35) in terms of the conjugate fields h_ϕ and $h_{S_{ij}}$ is not possible, nor the evaluation of the conjugate fields. Therefore we make a perturbation expansion of the kinetic coefficients (35) in h_ϕ and $h_{S_{ij}}$. Similar treatment was employed by Kawakatsu [7], who studied the effect of the change in the chain conformation on phase separation kinetics of block copolymer melts.

First we show the results of the zeroth-order calculations in h_ϕ and $h_{S_{ij}}$. That is, we replace the average in Eq. (33) by the average over the unperturbed Hamiltonian defined in Eq. (15). We also make a gradient expansion and to the second order in the gradients we obtain the following results:

$$\Lambda_{\phi\phi}(\mathbf{r},\mathbf{r}')=\frac{D_c v_0 N\bar{\phi}}{d}\mathcal{I}_2\left(\frac{dN}{2\epsilon}\right)\nabla'^2\delta(\mathbf{r}-\mathbf{r}'),\tag{36}$$

$$\Lambda_{\phi S_{ij}}(\mathbf{r},\mathbf{r}')=\frac{D_c v_0 N\bar{\phi}}{d^2}\left[\mathcal{I}_1\left(\frac{dN}{2\epsilon}\right)\right]^2\partial_i'\partial_j'\,\delta(\mathbf{r}-\mathbf{r}'),\tag{37}$$

$$\Lambda_{S_{ij}S_{kl}}(\mathbf{r},\mathbf{r}')=\frac{D_c v_0 N\bar{\phi}}{d^3}\Biggl\{\left[-\frac{2d^2}{\epsilon Nb^2}\mathcal{I}_1\left(\frac{dN}{\epsilon}\right)+e^{-dN/\epsilon}\mathcal{I}_2\left(\frac{dN}{2\epsilon}\right)\nabla'^2\right](\delta_{ik}\delta_{jl}+\delta_{il}\delta_{jk})+2e^{-dN/2\epsilon}\left[\mathcal{I}_1\left(\frac{dN}{2\epsilon}\right)\right]^2(\delta_{jl}\partial_i'\partial_k'+\delta_{jk}\partial_i'\partial_l'+\delta_{il}\partial_j'\partial_k'+\delta_{ik}\partial_j'\partial_l')\Biggr\}\,\delta(\mathbf{r}-\mathbf{r}'),\tag{38}$$

where $\nabla'\equiv\partial/\partial\mathbf{r}'$, $\partial_i'\equiv\partial/\partial r_i'$, and $\bar{\phi}$ is the average volume fraction of the polymers. We have defined

$$\mathcal{I}_n(x)=\frac{n!}{(-x)^n}\left(e^{-x}-\sum_{k=0}^{n-1}\frac{(-x)^k}{k!}\right), \tag{39}$$

and note that $\mathcal{I}_n(dN/\epsilon),\mathcal{I}_n(dN/2\epsilon)\to 1$ for the rigid rod limit $\epsilon/N\to\infty$. The detail of the calculation is given in Appendix A.

Next we proceed to the first order calculation in the conjugate fields. Although we can make such calculation for $\Lambda_{\phi S_{ij}}$ and $\Lambda_{S_{ij}S_{kl}}$, their resultant form is quite complicated and the physical meaning for their modification due to h_ϕ and $h_{S_{ij}}$ is not clear. Therefore we show the result only for $\Lambda_{\phi\phi}$ and we will discuss below the physical meaning of the modification of $\Lambda_{\phi\phi}$. The detail of the calculation is given in Appendix B and the result is given by

$$\begin{aligned}\Lambda_{\phi\phi}(\boldsymbol{r},\boldsymbol{r}')=\frac{D_c v_0 N\overline{\phi}}{d}\Bigg\{&\mathcal{I}_2\left(\frac{dN}{2\epsilon}\right)\nabla'^2\delta(\boldsymbol{r}-\boldsymbol{r}')\\&-\mathcal{I}_2\left(\frac{dN}{2\epsilon}\right)\partial'_i\overline{h}_\phi(\boldsymbol{r}')\partial'_i\,\delta(\boldsymbol{r}-\boldsymbol{r}')\\&-\left[\frac{4}{3}\mathcal{I}_3\left(\frac{dN}{\epsilon}\right)-\frac{4}{3}\mathcal{I}_3\left(\frac{dN}{2\epsilon}\right)+\mathcal{I}_2\left(\frac{dN}{2\epsilon}\right)\right]\\&\times\partial'_j(\overline{h}_{S_{ij}}(\boldsymbol{r}')\partial'_i\,\delta(\boldsymbol{r}-\boldsymbol{r}'))\Bigg\},\end{aligned} \tag{40}$$

where

$$\overline{h}_\phi(\boldsymbol{r})=v_0Nh_\phi(\boldsymbol{r}), \tag{41}$$

$$\overline{h}_{S_{ij}}(\boldsymbol{r})=\frac{v_0N}{d}(h_{S_{ij}}(\boldsymbol{r})+h_{S_{ji}}(\boldsymbol{r})). \tag{42}$$

III. SIMULATION

Since our model given in Sec. II is quite complicated, analytical treatment is difficult. Therefore we numerically integrate the kinetic equations for the order parameters. We restrict ourselves to the rigid rod case ($\epsilon/N\to\infty$) and we introduce dimensionless length $\tilde{x}=x/Nb$ and time $\tilde{t}=t/[d(Nb)^2/D_c\overline{\phi}]$. The dimensionless spatial derivative is $\tilde{\partial}_i=Nb\partial_i$. Then the free energy given in Eq. (21) can be rewritten as

$$\begin{aligned}F=\frac{1}{Nv_0\beta}\int d\boldsymbol{r}\Bigg\{&\phi\ln\phi+\frac{N}{N'}(1-\phi)\ln(1-\phi)\\&+\chi N\phi(1-\phi)-\frac{\phi}{2}\mathrm{Tr}\{\ln(\mathsf{1}+d\mathsf{Q})-d\mathsf{Q}\}\\&-\tfrac{1}{2}wN\phi^2\mathrm{Tr}(\mathsf{Q}-(\mathsf{1}/d)\mathrm{Tr}\,\mathsf{Q})^2+\tfrac{1}{2}WN\phi(\mathrm{Tr}\,\mathsf{Q})^2\\&+\frac{1}{2\phi}\tilde{C}_0(\tilde{\partial}_i\phi)^2+\tilde{L}_0\left(\tilde{\partial}_i\phi\tilde{\partial}_jQ_{ij}+\frac{1}{2\phi}Q_{ij}\tilde{\partial}_i\phi\tilde{\partial}_j\phi\right)\\&+\tfrac{1}{2}\tilde{L}_1\phi(\tilde{\partial}_kQ_{ij})^2+\tfrac{1}{2}\tilde{L}_2\phi\tilde{\partial}_iQ_{ij}\tilde{\partial}_kQ_{kj}\Bigg\},\end{aligned} \tag{43}$$

where $\tilde{C}_0=1/12d$, $\tilde{L}_0=1/12$, $L_1=d/24$, $\tilde{L}_2=d/6$ and the term proportional to $\tilde{L}_2$ has been changed for simplicity. We also introduce the dimensionless free energy $\tilde{F}=Nv_0\beta F$ and the dimensionless random noise terms $\tilde{\xi}_\phi=[d(Nb)^2/D_c\overline{\phi}]\xi_\phi$ and $\tilde{\xi}_{S_{ij}}=[d(Nb)^2/D_c\overline{\phi}]\xi_{S_{ij}}$. The equations of motion for the order parameters can be rewritten by using Eqs. (31), (32), (40) [or Eq. (36) when we do not consider the fields h_ϕ and $h_{S_{ij}}$], (37), and (38) and taking the rigid rod limit $\epsilon/N\to\infty$. The resultant equations are

$$\begin{aligned}\frac{\partial}{\partial t}\phi(\boldsymbol{r})=\partial_\mu&\left\{(\partial_\mu+(\partial_\mu\overline{h}_\phi)-\overline{h}_{S_{\mu\nu}}\partial_\nu)\frac{\delta F}{\delta\phi(\boldsymbol{r})}\right\}\\&+\frac{2}{d}\partial_\mu\partial_\nu\frac{\delta F}{\delta S_{\mu\nu}(\boldsymbol{r})}+\xi_\phi,\end{aligned} \tag{44}$$

$$\begin{aligned}\frac{\partial}{\partial t}S_{ij}(\boldsymbol{r})=\frac{2}{d}\partial_i\partial_j\frac{\delta F}{\delta\phi(\boldsymbol{r})}+\frac{2}{d^2}\Bigg[&\nabla^2\frac{\delta F}{\delta S_{ij}(\boldsymbol{r})}\\&+2\left(\partial_i\partial_\mu\frac{\delta F}{\delta S_{j\mu}(\boldsymbol{r})}+\partial_j\partial_\mu\frac{\delta F}{\delta S_{i\mu}(\boldsymbol{r})}\right)\Bigg]+\xi_{S_{ij}}.\end{aligned} \tag{45}$$

Hereafter all the tildes are omitted for brevity. Since we take only the first-order terms in h_ϕ and $h_{S_{ij}}$, in the simulation we retain only the first-order terms in Q_{ij} for these conjugate fields. Therefore, using Eqs. (18) and (19), we take

$$\overline{h}_\phi(\boldsymbol{r})=-\ln\phi(\boldsymbol{r}), \tag{46}$$

$$\overline{h}_{S_{ij}}(\boldsymbol{r})=-dQ_{ij}(\boldsymbol{r}). \tag{47}$$

Before presenting the results of our simulation, we make some remarks on these kinetic equations. When we deal with rigid rodlike polymers and allow them to move only translationally, which is the case in the biased reptation model, the orientational order behaves as a conserved variable [21] and in Eq. (45), S_{ij} is conserved. The orientational order is not actually conserved because of the rotational motion of the polymers, which is not incorporated in the biased reptation model as noted in Sec. II D. In a nondilute solution that we are interested in, rotational diffusion is suppressed due to the topological constraint imposed by surrounding chains. In a semidilute solution, $D_r/[D_c/(Nb)^2]\sim O(N^{-6})\ll 1$ [20], where D_r is the rotational diffusion constant, and our model can be considered as a limit $D_r/[D_c/(Nb)^2]\to 0$. To introduce the rotational diffusion phenomenologically, we can add a term like $-\tau_r^{-1}\delta F/\delta S_{ij}$ to the right hand side of Eq. (45), where $\tau_r^{-1}\simeq D_r/[D_c/(Nb)^2]\ll 1$.

Next we make a comment on the kinetic coefficient $\Lambda_{\phi\phi}$. The first term in the right-hand side of Eq. (44) can be rewritten as $-\boldsymbol{\nabla}\cdot\boldsymbol{J}_{\phi\phi}(\boldsymbol{r})$ with

$$(J_{\phi\phi}(\boldsymbol{r}))_i=\left\{-(\delta_{ij}+dQ_{ij}(\boldsymbol{r}))\partial_j+\frac{\partial_i\phi(\boldsymbol{r})}{\phi(\boldsymbol{r})}\right\}\frac{\delta F}{\delta\phi(\boldsymbol{r})}, \tag{48}$$

where use has been made of Eqs. (46) and (47). The first term in Eq. (48) states that polymers have a stronger tendency to diffuse parallel to the nematic orientation. This anisotropic diffusion can be incorporated in our model by

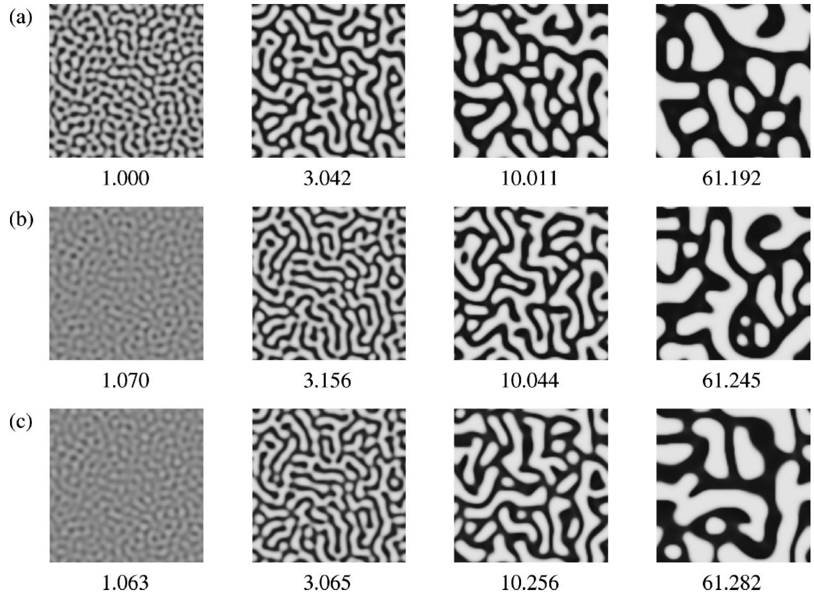

FIG. 1. Time evolution of the phase separation for (a) case 1, (b) case 2, and (c) case 3 with $wN=3$. The darkness represents ϕ. The numbers are times after quench. Under the same initial conditions.

evaluating the kinetic coefficient $\Lambda_{\phi\phi}$ in terms of the conjugate field $h_{S_{ij}}$. Without $h_{S_{ij}}$ and h_ϕ, $\Lambda_{\phi\phi}$ produces only the isotropic diffusion $\nabla^2 \delta F/\delta\phi$.

We numerically integrate Eqs. (44) and (45) on a two-dimensional 128×128 square lattice with the periodic boundary conditions using the Euler scheme. In all our simulations, we choose the parameters $\chi N=2.7$, and $WN=5$. The average volume fraction of the polymer is set equal to $\overline{\phi}=0.5$. To avoid numerical difficulties L_0 and $h_{S_{ij}}$ are multiplied by 0.7. We also set $N=N'$ for simplicity and to avoid numerical difficulties arising from the smallness of ϕ when we set $N\gg N'$. The lattice size and the time step are taken to be $\Delta x=0.25$ and $\Delta t=\Delta t_0\phi_{min}$, respectively, where ϕ_{min} is the minimum value of ϕ and Δt_0 will be specified below. We neglect the random noise terms ξ_ϕ and $\xi_{S_{ij}}$ in the kinetic equations which we believe will not have a significant effect on late stage phase separation kinetics. As the initial conditions, ϕ and Q_{ij} at each lattice points are random numbers uniformly distributed in $[\overline{\phi}-0.01,\overline{\phi}+0.01]$ and $[-0.01,0.01]$, respectively. That is, the initial conditions are homogeneous and isotropic with no orientational order.

We set the anisotropic interaction parameter to $wN=3$ or 5. We take $\Delta t_0=0.0002$ for $wN=3$ and $\Delta t_0=0.000\,15$ for $wN=5$. Note that phase separation into an isotropic phase poor in LCP's and a nematic phase rich in LCP's occurs in our simulations as mentioned in Sec. II C and that the magnitude of the orientational order in a nematic phase becomes larger with increasing wN. We also note that the spinodal point for the orientational order is $Nw\overline{\phi}=2$ for $d=2$ (see Sec. IV). Therefore when we take $wN=5$, phase separation and growth of orientational order occur simultaneously at $t=0$ and when $wN=3$ the orientational order grows after the compositional phase separation.

Characteristic of our kinetic equations, together with the modification of $\Lambda_{\phi\phi}$, is the presence of the off-diagonal kinetic coefficient $\Lambda_{\phi S}$, which has been neglected in phenomenological studies [18,19] of phase separation with orientational order. To check how phase separation kinetics is influenced by the presence of $\Lambda_{\phi S}$ and the modification of $\Lambda_{\phi\phi}$, we consider the following three cases: (i) without $\Lambda_{\phi S}$ and with $h_\phi=h_{S_{ij}}=0$ in $\Lambda_{\phi\phi}$ (referred to as case 1 below), (ii) with $\Lambda_{\phi S}$ and with $h_\phi=h_{S_{ij}}=0$ in $\Lambda_{\phi\phi}$ (case 2) and (iii) with $\Lambda_{\phi S}$ and with h_ϕ and $h_{S_{ij}}$ in $\Lambda_{\phi\phi}$ given by Eqs. (46) and (47) (case 3). In Fig. 1 we show the time evolution of the phase separation with $wN=3$ for each case. In all the cases, we can observe the formation and coarsening of a percolated network structure rich in polymers (black regions) and polymer-poor (white) regions form isolated structures. Such a network structure has been observed in experiments of phase separation in systems containing LCP's [13,16,17]. We also note that such an asymmetric morphology has been obtained in numerical analyses of viscoelastic phase separation [9,10] and of phase separation in elastic materials [35]. We show in Fig. 2 the orientational order at $t=61.282$ in case 3. Orientational order of polymers parallel to the interface or the network structure can be observed. We note that orientational order parallel to the interface is preferable because of the coupling terms proportional to L_0 in the free energy (43) [25]. Although we do not show the figures, the same behavior for the orientational order can be observed also in cases 1 and 2.

To make a quantitative comparison of the growth of the order for the three cases, we show in Fig. 3 the time evolution of the quantities $\langle\delta\phi^2\rangle$ and $\langle\tilde{Q}_{ij}^2\rangle$, where $\delta\phi=\phi-\overline{\phi}$ and $\tilde{Q}_{ij}$ is the traceless part of Q_{ij}. We also check the time evolution of the characteristic lengths. As a characteristic length, we take a length determined by the interface length defined by

$$l_{int}(t)=\frac{A}{(\text{interface length at }\ t)},\tag{49}$$

where A is the area of the system. We also define another

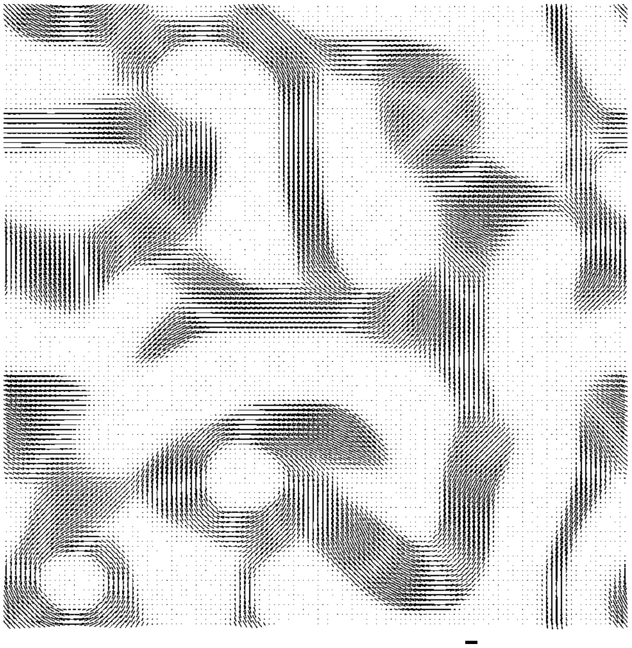

FIG. 2. Orientational order at $t=61.282$ in case 3 with $wN=3$. The length and the orientation of the lines represent S and n_i, respectively, where $\phi(Q_{ij}-Q_{kk}\delta_{ij}/2)=S(n_in_j-\delta_{ij}/2)$. The length of the thick solid line corresponds to $S=0.5598$, the maximum value of S in the figure.

characteristic length $l_k(t)=2\pi/\overline{k}(t)$, where $\overline{k}(t)$ is the average wavenumber defined as [36]

$$\overline{k}(t)=\frac{\int dk\, kS(k,t)}{\int dk\, S(k,t)}. \tag{50}$$

Here $S(k,t)$ is the circular average of the structure factor $S(\boldsymbol{k},t)=\langle|\phi(\boldsymbol{k},t)|^2\rangle$, $\phi(\boldsymbol{k},t)$ being the Fourier transform of $\phi(\boldsymbol{r},t)$. The time evolution of the characteristic lengths $l_{int}(t)$ and $l_k(t)$ is shown in Fig. 4. We find from Fig. 3 that the compositional order grows faster without $\Lambda_{\phi S}$ (case 1) than with $\Lambda_{\phi S}$ (cases 2 and 3), which can be seen also in Fig. 1. We also find from Figs. 3 and 4 that the characteristic lengths start to grow earlier without $\Lambda_{\phi S}$ than with $\Lambda_{\phi S}$ and that they start to grow when $\langle\delta\phi^2\rangle\simeq 0.22$. We will return to this problem in Sec. IV. At $t\gtrsim 15$, the characteristic lengths obey $l\sim t^{\alpha}$ with $\alpha\simeq 1/3$, which is a typical growth law for systems with conserved order parameters [1]. We can also observe a slightly faster growth in case 3 than in case 2 at $2\lesssim t\lesssim 10$.

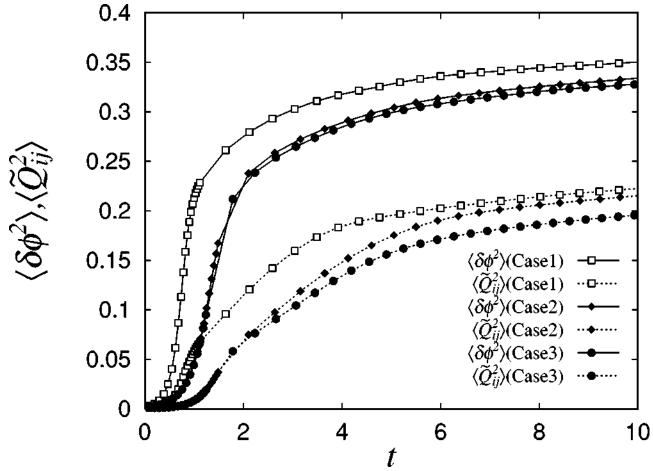

FIG. 3. Time evolution of $\langle\delta\phi^2\rangle$ and $\langle\tilde{Q}_{ij}^2\rangle$ for $wN=3$.

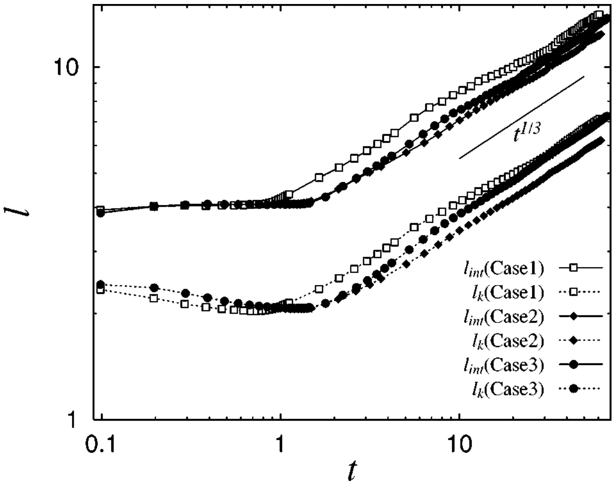

FIG. 4. Time evolution of the characteristic lengths $l_{int}(t)$ and $l_k(t)$ for $wN=3$.

Experiments on phase separation in mixtures of LCP's and flexible polymers show that an evaporation-condensation process of flexible-polymer-rich (LCP-poor) domains and a breakup process of a network structure rich in LCP's can be observed as a coarsening mechanism [16]. The coarsening processes in cases 2 and 3 are illustrated in Fig. 5. In our simulation both processes occur in case 3 and in cases 1 and 2 (although we have not shown case 1 in Fig. 5) only evaporation-condensation processes can be observed and the breakage of network structures rich in LCP's is quite rare. Therefore the breakage of a network is attributed to the tendency of LCP's to diffuse parallel to the nematic orientation, although in actual systems hydrodynamic flow induced by capillary pressure may play an important role (note that our model does not incorporate hydrodynamic effect).

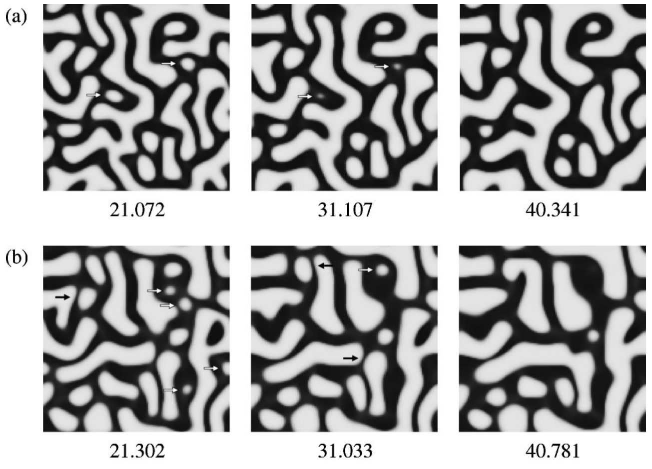

21.072 31.107 40.341

21.302 31.033 40.781

FIG. 5. Illustration of the coarsening process in cases 2 and 3 with $wN=3$. White arrows indicate the evaporation-condensation mechanism and black arrows indicate the breakage of a network structure.

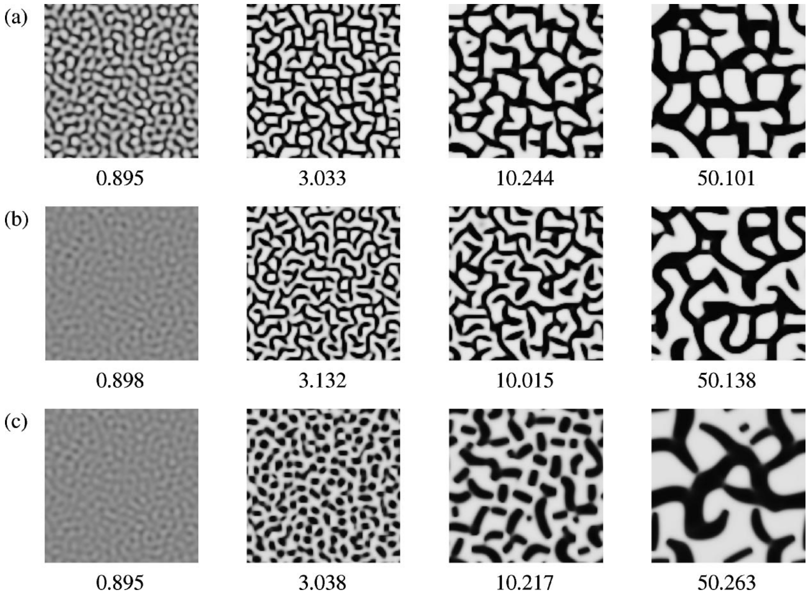

FIG. 6. Time evolution of the phase separation for (a) case 1, (b) case 2, and (c) case 3 with $wN=5$.

Next we show in Fig. 6 the time evolution of the compositional order with $wN=5$. While we also observe a network structure rich in LCP's in cases 1 and 2, droplet morphology can be observed in case 3. In case 3 breakup of the transient network structure occurs before $t\simeq 3$ and is shown in Fig. 7. We note that in experiments on phase separation in mixtures of LCP's and flexible polymers, formation of droplets after the breakup of the network structure is observed [16,17]. The process shown in Fig. 7 closely resembles that observed in experiments. We show in Fig. 8 the growth of the order as in Fig. 3. We find a faster growth of the compositional order without $\Lambda_{\phi S}$ than with $\Lambda_{\phi S}$ as in the cases with $wN=3$. We also find a faster growth of the orientational order than in the cases with $wN=3$ and the magnitude of the orientational order is larger than in $wN=3$. As mentioned above, the tendency of LCP's to diffuse parallel to the nematic orientation incorporated in case 3 tends to break up the network structure. In case 3 with $wN=5$, orientational order appears earlier than in $wN=3$ and its magnitude is so large that the transient structure observed in the early stage breaks up into droplets. We show in Fig. 9 the time evolution of the characteristic lengths $l_{int}(t)$ and $l_k(t)$. Although we can observe a typical growth for conserved systems $l\sim t^{1/3}$ for case 2, the growth in case 1 is slower than $l\sim t^{1/3}$ at $t\gtrsim 10$. We also find that the growth in case 3 is much faster than in case 2. We can conclude from Figs. 4 and 9 that in our model the tendency of LCP's to diffuse parallel to the nematic orientation incorporated in case 3 fastens the coarsening kinetics in late stages.

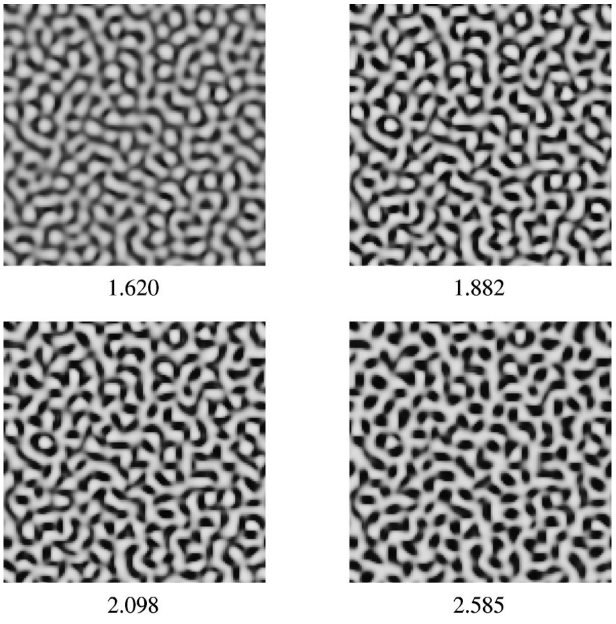

FIG. 7. Breakup of the transient network structure in case 3 with $wN=5$.

IV. LINEAR ANALYSIS OF THE GROWING MODE

The presence of the off-diagonal kinetic coefficient $\Lambda_{\phi S}$ together with the coupling of ϕ and S_{ij} in the free energy leads to the growth of the compositional order and the orientational order in a coupled fashion. To check how ϕ and S_{ij} evolve in the early stage, we perform a linear analysis of the growing modes from a homogeneous and isotropic state

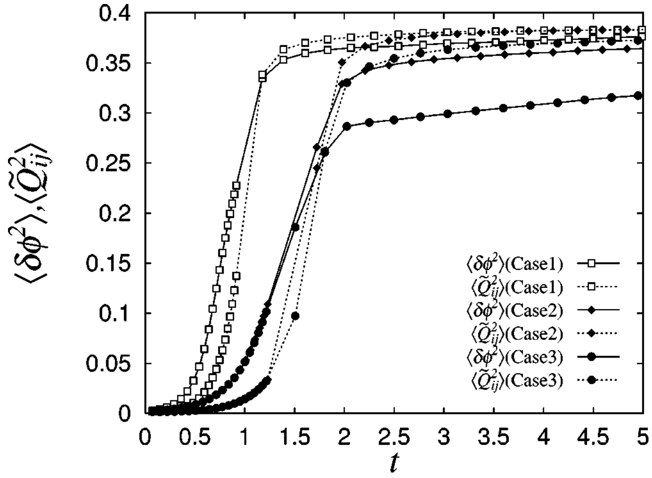

FIG. 8. Time evolution of $\langle\delta\phi^2\rangle$ and $\langle\tilde{Q}_{ij}^2\rangle$ for $wN=5$.

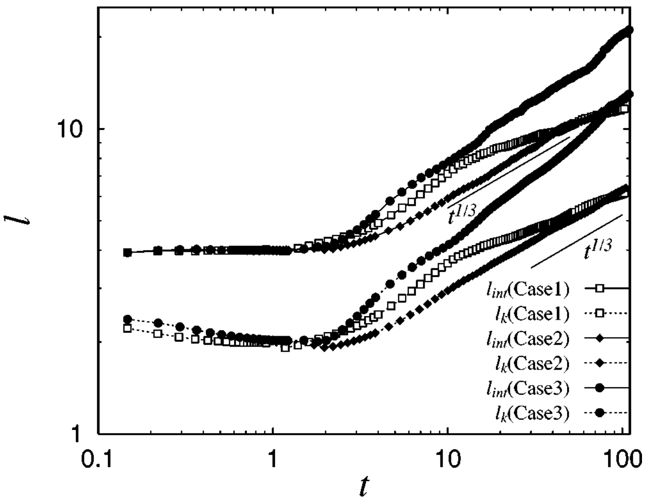

FIG. 9. Time evolution of the characteristic lengths $l_{int}(t)$ and $l_k(t)$ for $wN=5$.

$\delta\phi(\boldsymbol{r})=\phi(\boldsymbol{r})-\overline{\phi}=0$ and $Q_{ij}(\boldsymbol{r})=0$. The linearized equations are

$$\frac{\partial}{\partial t}\delta\phi_{\boldsymbol{q}}=-q^2\frac{\delta F}{\delta\phi}-p\frac{2q_kq_l}{d}\frac{\delta F}{\delta S_{kl}}, \tag{51}$$

$$\overline{\phi}\frac{\partial}{\partial t}\delta Q_{ij\boldsymbol{q}}=-p\frac{2q_iq_j}{d}\frac{\delta F}{\delta\phi}-\frac{2q^2}{d^2}\frac{\delta F}{\delta S_{ij}}-\frac{4}{d^2}\left(q_iq_k\frac{\delta F}{\delta S_{jk}}+q_jq_k\frac{\delta F}{\delta S_{ik}}\right), \tag{52}$$

where q_i is the wave number and $p=1$ with $\Lambda_{\phi S}$ (cases 2 and 3) and $p=0$ without $\Lambda_{\phi S}$ (case 1). The $\delta\phi_{\boldsymbol{q}}$ and $\delta Q_{ij\boldsymbol{q}}$ are the Fourier transform of $\delta\phi(\boldsymbol{r})$ and $\delta Q_{ij}(\boldsymbol{r})$, respectively. The linearized functional derivatives are

$$\frac{\delta F}{\delta\phi}=\left(A+\frac{C_0}{\overline{\phi}}q^2\right)\delta\phi_{\boldsymbol{q}}+L_0q_kq_l\delta Q_{kl\boldsymbol{q}}, \tag{53}$$

$$\frac{\delta F}{\delta S_{ij}}=\left(\frac{d^2}{2}-wN\overline{\phi}+L_1q^2\right)\delta Q_{ij\boldsymbol{q}}+\left(\frac{wN\overline{\phi}}{d}+WN\right)\delta_{ij}\delta Q_{kk\boldsymbol{q}}+\tfrac{1}{2}L_2(q_jq_k\delta Q_{ik\boldsymbol{q}}+q_iq_k\delta Q_{jk\boldsymbol{q}})+\frac{L_0}{\overline{\phi}}q_iq_j\delta\phi_{\boldsymbol{q}}, \tag{54}$$

with $A=1/\overline{\phi}+1/(1-\overline{\phi})-2\chi N$.

Since the initial state is isotropic, there is no preferred direction and we take the wave number $\boldsymbol{q}$ parallel to the z axis. Then we find four independent modes $\delta Q_{xx}-\delta Q_{yy}$, δQ_{xy}, δQ_{xz} and δQ_{yz}, the linearized equations for which can be written as

$$\overline{\phi}\frac{\partial}{\partial t}\delta Q_{ij\boldsymbol{q}}=-\frac{2q^2}{d^2}\left(\frac{d^2}{2}-wN\overline{\phi}+L_1q^2\right)\delta Q_{ij\boldsymbol{q}},\quad (\delta Q_{ij}=\delta Q_{xx}-\delta Q_{yy}\ \text{or}\ \delta Q_{xy}), \tag{55}$$

$$\overline{\phi}\frac{\partial}{\partial t}\delta Q_{ij\boldsymbol{q}}=-\frac{6q^2}{d^2}\left[\frac{d^2}{2}-wN\overline{\phi}+\left(L_1+\frac{1}{2}L_2\right)q^2\right]\delta Q_{ij\boldsymbol{q}},\quad (\delta Q_{ij}=\delta Q_{xz}\ \text{or}\ \delta Q_{yz}). \tag{56}$$

These four modes can grow when $wN\overline{\phi}>d^2/2$. The maximum growing rate is given by

$$\lambda^*=\frac{\left(wN\overline{\phi}-\frac{d^2}{2}\right)^2}{2d^2L_1\overline{\phi}}\quad (\text{for}\ \delta Q_{xx}-\delta Q_{yy}\ \text{and}\ \delta Q_{xy}), \tag{57}$$

$$\lambda^*=\frac{3\left(wN\overline{\phi}-\frac{d^2}{2}\right)^2}{d^2(2L_1+L_2)\overline{\phi}}\quad (\text{for}\ \delta Q_{xz}\ \text{and}\ \delta Q_{yz}), \tag{58}$$

and the corresponding wave number is

$$q^*=\sqrt{\frac{wN\overline{\phi}-\frac{d^2}{2}}{2L_1}}\quad (\text{for}\ \delta Q_{xx}-\delta Q_{yy}\ \text{and}\ \delta Q_{xy}), \tag{59}$$

$$q^*=\sqrt{\frac{wN\overline{\phi}-\frac{d^2}{2}}{2L_1+L_2}}\quad (\text{for}\ \delta Q_{xz}\ \text{and}\ \delta Q_{yz}). \tag{60}$$

We also find that $\delta\phi$, δQ_{zz} and δQ_{kk} evolve in a coupled manner and their time evolution can be described by

$$\frac{\partial}{\partial t}\delta\phi_{\boldsymbol{q}}=-q^2\left\{\left(A+\frac{C_0}{\overline{\phi}}q^2\right)\delta\phi_{\boldsymbol{q}}+L_0q^2\delta Q_{zz\boldsymbol{q}}\right\}-p\frac{2q^2}{d}\times\left\{\frac{L_0}{\overline{\phi}}q^2\delta\phi_{\boldsymbol{q}}+\left(\frac{d^2}{2}-wN\overline{\phi}+(L_1+L_2)q^2\right)\delta Q_{zz\boldsymbol{q}}+\left(\frac{wN\overline{\phi}}{d}+WN\right)\delta Q_{kk\boldsymbol{q}}\right\}, \tag{61}$$

$$\overline{\phi}\frac{\partial}{\partial t}\delta Q_{zz\boldsymbol{q}}=-p\frac{2q^2}{d}\left\{\left(A+\frac{C_0}{\overline{\phi}}q^2\right)\delta\phi_{\boldsymbol{q}}+L_0q^2\delta Q_{zz\boldsymbol{q}}\right\}-\frac{10q^2}{d^2}\left\{\frac{L_0}{\overline{\phi}}q^2\delta\phi_{\boldsymbol{q}}+\left(\frac{d^2}{2}-wN\overline{\phi}+(L_1+L_2)q^2\right)\delta Q_{zz\boldsymbol{q}}+\left(\frac{wN\overline{\phi}}{d}+WN\right)\delta Q_{kk\boldsymbol{q}}\right\}, \tag{62}$$

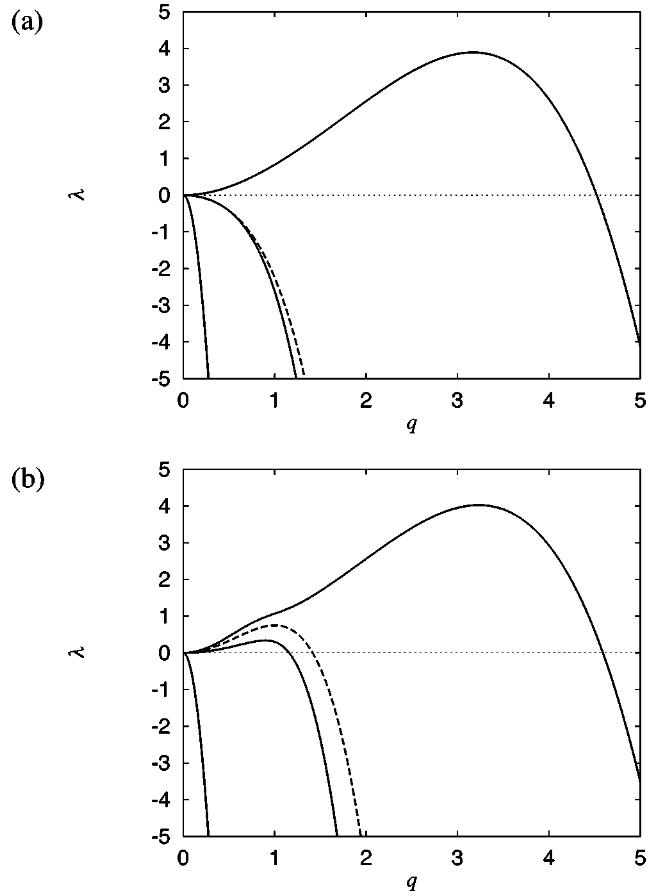

FIG. 10. Growth rate λ of the coupled mode of $\delta\phi, \delta Q_{zz}$ and δQ_{kk} for (a) $wN=3$ and (b) $wN=5$ is shown by three solid lines. We also show the growth rate of δQ_{xz} by dashed lines for reference.

$$\bar{\phi}\frac{\partial}{\partial t}\delta Q_{kk\mathbf{q}} = -p\frac{2q^2}{d}\left\{\left(A+\frac{C_0}{\bar{\phi}}q^2\right)\delta\phi_{\mathbf{q}} + L_0 q^2\delta Q_{zz\mathbf{q}}\right\} - \frac{8q^2}{d^2}\left\{\frac{5L_0}{4\bar{\phi}}q^2\delta\phi_{\mathbf{q}} + \left[\frac{d^2}{2} - wN\bar{\phi} + \left(L_1+\frac{5}{4}L_2\right)q^2\right]\delta Q_{zz\mathbf{q}} + \left[\frac{d^2}{8}+\frac{wN\bar{\phi}}{d} + \left(1+\frac{d}{4}\right)WN + \frac{1}{4}L_1 q^2\right]\delta Q_{kk\mathbf{q}}\right\}. \tag{63}$$

Similar results have been obtained in Refs. [21] and [22]. We show in Fig. 10 the growth rate λ of this coupled mode as a function of the magnitude of the wave number q for $wN=3$ and 5 with $p=1$ (with $\Lambda_{\phi S}$) and the other parameters used in our simulations. The most stable mode with negative λ for all $q>0$ is associated with the fluctuation of the segment length or trace of Q_{ij}, and the intermediate mode, stable for $wN=3$ and unstable for $wN=5$, is related to the orientational order. Note that the spinodal point for orientational order is $wN=d^2/2\bar{\phi}=4$ because in our simulation $d=2$ and we set $\bar{\phi}=0.5$. The most unstable mode represents the growth of the compositional order $\delta\phi$. Note that the growth rate of all the modes at $q=0$ is zero because the orientational order as well as the compositional order behaves as a conserved variable in our model(see Sec. III).

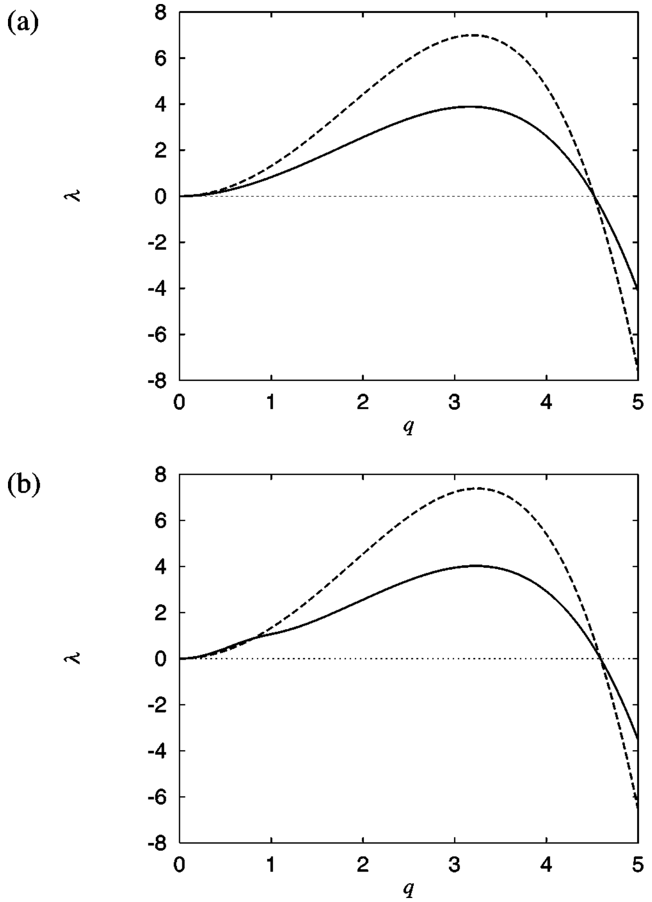

FIG. 11. Growth rate λ of the coupled mode of $\delta\phi, \delta Q_{zz}$ and δQ_{kk} for (a) $wN=3$ and (b) $wN=5$. The solid line represents the case with $\Lambda_{\phi S}(p=1)$ and the dashed line without $\Lambda_{\phi S}(p=0)$. Only the most unstable mode associated with the compositional order is shown.

We show in Fig. 11 the growth rate of the most unstable mode associated with the compositional order $\delta\phi$ for the cases with $\Lambda_{\phi S}(p=1)$ and without $\Lambda_{\phi S}$ $(p=0)$. The maximum growing rate λ^* and the corresponding wave number q^* are shown in Table I. The wave number of the mode with the maximum growing rate is not significantly different between the cases without and with $\Lambda_{\phi S}$, while the maximum growth rate is smaller with $\Lambda_{\phi S}$ than without $\Lambda_{\phi S}$, which is responsible for the slow growth of the compositional order with $\Lambda_{\phi S}$ observed in our simulation. We note that the suppression of the compositional order in the early stage of the

TABLE I. Maximum growing rate λ^* and the corresponding wave number q^* of the mode associated with the compositional order.

	λ^*		q^*	
wN	without $\Lambda_{\phi S}$	with $\Lambda_{\phi S}$	without $\Lambda_{\phi S}$	with $\Lambda_{\phi S}$
3	7.00	3.89	3.20	3.16
5	7.39	4.02	3.24	3.24

phase separation due to the off-diagonal coupling with another degree of freedom has been observed in a numerical analysis of the viscoelastic phase separation [9,10].

V. CONCLUSION

In this paper we have investigated phase separation kinetics of main-chain LCP's by numerically solving the coupled time-dependent Ginzburg-Landau equations for the compositional order parameter ϕ and the orientational order parameter S_{ij}. The kinetic coefficients are calculated by using the biased reptation model and one of the coefficients $\Lambda_{\phi\phi}$ is evaluated by a perturbation expansion in self-consistent fields h_ϕ and $h_{S_{ij}}$ conjugate to the order parameters. By this treatment we can incorporate the tendency of LCP's to diffuse parallel to the nematic orientation. We have shown that the phase separation leads to a network structure rich in polymers and that the orientation of the polymers is parallel to the interface between polymer-rich regions and polymer-poor regions. The presence of the off-diagonal kinetic coefficient $\Lambda_{\phi S}$ suppresses the growth of the compositional order in the early stage, which has been shown by a linear analysis of the growing modes. We have also shown that the tendency of the polymers to diffuse parallel to the nematic orientation causes the breakage of the network structure. In conclusion, the coupling between compositional order and orientational order in the kinetics as well as in the free energy plays a significant role in phase separation and domain morphology in LCP's.

ACKNOWLEDGMENTS

The author is grateful to Professor Akira Onuki, Professor Toshihiro Kawakatsu, Dr. Hiroya Kodama, and Takeaki Araki for helpful discussions and comments. Part of the numerical computation in this work was carried out at the Yukawa Institute Computer Facility. This work was partially supported by a Grant-in-Aid for Scientific Research from the Ministry of Education, Science and Culture.

APPENDIX A: ZEROTH-ORDER CALCULATION OF THE KINETIC COEFFICIENTS

In this Appendix we calculate the kinetic coefficients up to zeroth order in the conjugate fields h_ϕ and $h_{S_{ij}}$. First we rewrite Eq. (33) as

$$\begin{aligned}\Lambda_{\psi_1\psi_2}(\boldsymbol{r},\boldsymbol{r}') = -D_c n\{&\langle\hat{\psi}_1(L,\boldsymbol{r})\hat{\psi}_2(L,\boldsymbol{r}')\rangle \\ &+\langle\hat{\psi}_1(0,\boldsymbol{r})\hat{\psi}_2(0,\boldsymbol{r}')\rangle-\langle\hat{\psi}_1(0,\boldsymbol{r})\hat{\psi}_2(L,\boldsymbol{r}')\rangle \\ &-\langle\hat{\psi}_1(L,\boldsymbol{r})\hat{\psi}_2(0,\boldsymbol{r}')\rangle\}, \\ &(\psi_1,\psi_2=\phi \text{ or } S_{ij}). \quad \text{(A1)}\end{aligned}$$

Here we replace the average in Eq. (A1) by the average defined in Eq. (15). By using Eqs. (2) and (A1), the coefficient $\Lambda_{\phi\phi}$ can be rewritten as

$$\begin{aligned}\Lambda_{\phi\phi}(\boldsymbol{r},\boldsymbol{r}') = -\frac{D_c n v_0^2}{b^2 V}(2\delta(\boldsymbol{r}-\boldsymbol{r}') &-\langle\delta(r-\boldsymbol{r}'-[\boldsymbol{R}(0)-\boldsymbol{R}(L)])\rangle_0 \\ &-\langle\delta(r-\boldsymbol{r}'-[\boldsymbol{R}(L)-\boldsymbol{R}(0)])\rangle_0), \quad \text{(A2)}\end{aligned}$$

where V is the volume of the system. Using the Fourier transform we can derive

$$\begin{aligned}&\langle\delta(r-\boldsymbol{r}'-[\boldsymbol{R}(0)-\boldsymbol{R}(L)])\rangle_0 \\ &=\frac{1}{(2\pi)^d}\int d\boldsymbol{q}\, e^{-i\boldsymbol{q}\cdot(\boldsymbol{r}-\boldsymbol{r}')}\langle\exp\{-i\boldsymbol{q}\cdot[\boldsymbol{R}(L)-\boldsymbol{R}(0)]\}\rangle_0 \\ &=\frac{1}{(2\pi)^d}\int d\boldsymbol{q}\, e^{-i\boldsymbol{q}\cdot(\boldsymbol{r}-\boldsymbol{r}')} \\ &\quad\times\{\exp(-\tfrac{1}{2}q_iq_j\langle[R_i(L)-R_i(0)][R_j(L)-R_j(0)]\rangle_0\}, \quad \text{(A3)}\end{aligned}$$

where we have utilized the fact that $\boldsymbol{R}$ is a variable with a Gaussian distribution. To evaluate the average appearing in Eq. (A3), we make a normal mode analysis [25,31]. The Fourier transform of $\boldsymbol{R}(\tau)$ is

$$\boldsymbol{R}_\xi=\frac{1}{\sqrt{2\pi}}\int_{-\infty}^{\infty}d\tau\,\boldsymbol{R}(\tau)e^{-i\xi\tau}, \quad \text{(A4)}$$

where summation over ξ is replaced by an integral, supposing an infinite chain. This treatment greatly simplifies the calculation because we can neglect the inhomogeneity at the chain ends. From the wormlike-chain Hamiltonian (7) and Eq. (8), we obtain

$$\langle R_{i\xi}R_{j\xi'}\rangle_0=\frac{1}{\left(\dfrac{d^2}{4\epsilon b}+\epsilon b\xi^2\right)\xi^2}\delta_{ij}\delta(\xi+\xi'). \quad \text{(A5)}$$

Using Eq. (A5), we can calculate the average appearing in Eq. (A3) and the result is

$$\langle[R_i(L)-R_i(0)][R_j(L)-R_j(0)]\rangle_0=\delta_{ij}\frac{L^2}{d}\mathcal{I}_2\left(\frac{dN}{2\epsilon}\right), \quad \text{(A6)}$$

where $\mathcal{I}_2$ has been defined in Eq. (39). From Eqs. (A2), (A3), and (A6) we obtain $L_{\phi\phi}$ and expanding Eq (A3) in $\boldsymbol{q}$ (equivalent to the gradient expansion) and taking the terms up to second order in $\boldsymbol{q}$, we finally obtain Eq. (36) (notice that the average volume fraction of polymers is $\bar{\phi}=v_0Nn/V$).

We can also calculate $\Lambda_{\phi S_{ij}}$ and $\Lambda_{S_{ij}S_{kl}}$ in a similar way by noticing that

$$\left\langle u_i(\tau)u_j(\tau)-\frac{1}{d}\delta_{ij}\right\rangle_0=0, \quad \text{(A7)}$$

$$\begin{aligned}&\left\langle\left(u_i(L)u_j(L)-\frac{1}{d}\delta_{ij}\right)[R_k(L)-R_k(0)][R_l(L)-R_l(0)]\right\rangle_0\\&\quad=\left[\frac{L}{d}\mathcal{I}_1\left(\frac{dN}{2\epsilon}\right)\right]^2(\delta_{ik}\delta_{jl}+\delta_{il}\delta_{jk}),\end{aligned}\tag{A8}$$

$$\begin{aligned}&\left\langle\left(u_i(0)u_j(0)-\frac{1}{d}\delta_{ij}\right)\left(u_k(0)u_l(0)-\frac{1}{d}\delta_{ij}\right)\right\rangle_0\\&\quad=\frac{1}{d^2}(\delta_{ik}\delta_{jl}+\delta_{il}\delta_{jk}),\end{aligned}\tag{A9}$$

$$\begin{aligned}&\left\langle\left(u_i(0)u_j(0)-\frac{1}{d}\delta_{ij}\right)\left(u_k(L)u_l(L)-\frac{1}{d}\delta_{ij}\right)\right\rangle_0\\&\quad=\frac{1}{d^2}e^{-dN/\epsilon}(\delta_{ik}\delta_{jl}+\delta_{il}\delta_{jk}),\end{aligned}\tag{A10}$$

$$\begin{aligned}&\left\langle\left(u_i(L)u_j(L)-\frac{1}{d}\delta_{ij}\right)\left(u_k(L)u_l(L)-\frac{1}{d}\delta_{kl}\right)\right.\\&\qquad\left.\times[R_\mu(L)-R_\mu(0)][R_\nu(L)-R_\nu(0)]\right\rangle_0\\&\quad=\frac{L^2}{d^3}\left\{e^{-dN/\epsilon}\mathcal{I}_2\left(\frac{dN}{2\epsilon}\right)\delta_{\mu\nu}(\delta_{ik}\delta_{jl}+\delta_{il}\delta_{jk})\right.\\&\qquad+e^{-dN/2\epsilon}\left[\mathcal{I}_1\left(\frac{dN}{2\epsilon}\right)\right]^2(\delta_{i\mu}(\delta_{k\nu}\delta_{jl}+\delta_{l\nu}\delta_{jk})\\&\qquad+\delta_{j\mu}(\delta_{k\nu}\delta_{il}\quad+\delta_{l\nu}\delta_{ik})+\delta_{k\mu}(\delta_{j\nu}\delta_{il}+\delta_{i\nu}\delta_{jl})\\&\qquad\left.+\delta_{l\mu}(\delta_{j\nu}\delta_{ik}+\delta_{i\nu}\delta_{jk}))\right\}.\end{aligned}\tag{A11}$$

Equations (A7), (A8), (A9), (A10), and (A11) can be obtained by using Eqs. (A4) and (A5).

APPENDIX B: CALCULATION OF THE KINETIC COEFFICIENT $\Lambda_{\phi\phi}$ FIRST ORDER IN THE CONJUGATE FIELDS

Here we show the calculation of the kinetic coefficient $\Lambda_{\phi\phi}$ as a perturbation expansion up to first order in the conjugate fields h_ϕ and $h_{S_{ij}}$. In this calculation, $\Lambda_{\phi\phi}$ is also given by Eq. (A2), where the average should be replaced as

$$\begin{aligned}&\langle\delta(\boldsymbol{r}-\boldsymbol{r}'-[\boldsymbol{R}(0)-\boldsymbol{R}(L)])\rangle\\&\quad\simeq\langle\delta(r-\boldsymbol{r}'-[\boldsymbol{R}(0)-\boldsymbol{R}(L)])\rangle_0(1+\langle\beta\mathcal{H}_1\rangle_0)\\&\qquad-\langle\delta(r-\boldsymbol{r}'-[\boldsymbol{R}(0)-\boldsymbol{R}(L)])\beta\mathcal{H}_1\rangle_0,\end{aligned}\tag{B1}$$

which can be obtained by making a perturbation expansion of Eq. (35) in terms of the interaction Hamiltonian $\mathcal{H}_1$. By using Eqs. (2), (4), and (9), the last term in Eq. (B1) can be written as

$$\begin{aligned}&\langle\delta(r-\boldsymbol{r}'-[\boldsymbol{R}(0)-\boldsymbol{R}(L)])\beta\mathcal{H}_1\rangle_0\\&\quad=\frac{1}{(2\pi)^{2d}}\int d\boldsymbol{q}\int d\boldsymbol{q}'e^{-i\boldsymbol{q}\cdot(\boldsymbol{r}-\boldsymbol{r}')}e^{-i\boldsymbol{q}'\cdot\boldsymbol{r}'}\frac{v_0}{b}\int_0^L d\tau\\&\qquad\times\left\langle e^{i\boldsymbol{q}\cdot(\boldsymbol{R}(0)-\boldsymbol{R}(L))}e^{-i\boldsymbol{q}'\cdot(\boldsymbol{R}(\tau)-\boldsymbol{R}(L))}\right.\\&\qquad\left.\times\left\{h_\phi(\boldsymbol{q}')+\left(u_i(\tau)u_j(\tau)-\frac{1}{d}\delta_{ij}\right)h_{S_{ij}}(\boldsymbol{q}')\right\}\right\rangle_0,\end{aligned}\tag{B2}$$

where we have introduced the Fourier transform

$$h_\psi(\boldsymbol{q})=\int d\boldsymbol{r}\,e^{i\boldsymbol{q}\cdot\boldsymbol{r}}h_\psi(\boldsymbol{r}),\quad(\psi=\phi\ \text{or}\ S_{ij}).\tag{B3}$$

We make an expansion in terms of the wave numbers $\boldsymbol{q}$ and $\boldsymbol{q}'$ as in Appendix A and we also here retain the second-order terms in the wave numbers. Then the average in Eq. (B2) is

$$\begin{aligned}&\langle\cdots\rangle_0\simeq(\text{zeroth-order terms in }\boldsymbol{q})+q_kq_l'\Bigl\{\langle[R_k(0)-R_k(L)]\\&\qquad\times[R_l(\tau)-R_l(L)]\rangle_0h_\phi(\boldsymbol{q}')+\Bigl\langle[R_k(0)-R_k(L)]\\&\qquad\times[R_l(\tau)-R_l(L)]\left(u_i(\tau)u_j(\tau)-\frac{1}{d}\delta_{ij}\right)\Bigr\rangle_0h_{S_{ij}}(\boldsymbol{q}')\Bigr\}\\&\qquad-\tfrac{1}{2}q_kq_l\Bigl\{\langle[R_k(0)-R_k(L)][R_l(0)\\&\qquad-R_l(L)]\rangle_0h_\phi(\boldsymbol{q}')+\Bigl\langle(R_k(0)-R_k(L))\Bigl(R_l(0)\\&\qquad-R_l(L))\left(u_i(\tau)u_j(\tau)-\frac{1}{d}\delta_{ij}\right)\Bigr\rangle_0h_{S_{ij}}(\boldsymbol{q}')\Bigr\}.\end{aligned}\tag{B4}$$

Zeroth order terms in $\boldsymbol{q}$ yield $\delta(\boldsymbol{r}-\boldsymbol{r}')\langle\beta\mathcal{H}_1\rangle_0$ and eventually cancel out by the first term in the right-hand side of Eq. (B1). Evaluating the averages in Eq. (B4), we obtain

$$\begin{aligned}&\langle\delta(r-\boldsymbol{r}'-[\boldsymbol{R}(0)-\boldsymbol{R}(L)])\beta\mathcal{H}_1\rangle_0\\&\quad=\frac{1}{(2\pi)^{2d}}\int d\boldsymbol{q}\int d\boldsymbol{q}'e^{-i\boldsymbol{q}\cdot(\boldsymbol{r}-\boldsymbol{r}')}e^{-i\boldsymbol{q}'\cdot\boldsymbol{r}'}\frac{v_0}{b}\\&\qquad\times\Biggl(q_kq_l'\Biggl\{\frac{L^3}{2d}\mathcal{I}_2\left(\frac{dN}{2\epsilon}\right)\delta_{kl}h_\phi(\boldsymbol{q}')+\frac{L^3}{d^2}\Biggl[\frac{2}{3}\mathcal{I}_3\left(\frac{dN}{\epsilon}\right)\\&\qquad-\frac{2}{3}\mathcal{I}_3\left(\frac{dN}{2\epsilon}\right)+\frac{1}{2}\mathcal{I}_2\left(\frac{dN}{2\epsilon}\right)\Biggr](\delta_{ik}\delta_{jl}+\delta_{il}\delta_{jk})h_{S_{ij}}(\boldsymbol{q}')\Biggr\}\\&\qquad-\frac{1}{2}q_kq_l\Biggl\{\delta_{kl}\frac{L^3}{d}\mathcal{I}_2\left(\frac{dN}{2\epsilon}\right)h_\phi(\boldsymbol{q}')+\frac{L^3}{d^2}\Biggl[\frac{4}{3}\mathcal{I}_3\left(\frac{dN}{\epsilon}\right)\\&\qquad-\frac{4}{3}\mathcal{I}_3\left(\frac{dN}{2\epsilon}\right)+\mathcal{I}_2\left(\frac{dN}{2\epsilon}\right)\Biggr](\delta_{ik}\delta_{jl}+\delta_{il}\delta_{jk})h_{S_{ij}}(\boldsymbol{q}l')\Biggr\}\Biggr).\end{aligned}\tag{B5}$$

The first term in Eq. (B1) is evaluated to be

$$\begin{aligned}\langle \delta(r-\boldsymbol{r}'-[\boldsymbol{R}(0)-\boldsymbol{R}(L)])\rangle_0(1+\langle\beta\mathcal{H}_1\rangle_0)\\ \simeq\left\{1+\frac{L^2}{2d}\mathcal{I}_2\left(\frac{dN}{2\epsilon}\right)\nabla'^2\right\}\delta(\boldsymbol{r}-\boldsymbol{r}')\\ +\langle\beta\mathcal{H}_1\rangle_0\delta(\boldsymbol{r}-\boldsymbol{r}')\\ +\frac{L^2}{2d}\mathcal{I}_2\left(\frac{dN}{2\epsilon}\right)\langle\beta\mathcal{H}_1\rangle_0\nabla'^2\delta(\boldsymbol{r}-\boldsymbol{r}'),\end{aligned} \tag{B6}$$

where we have used the results in Appendix A and retained up to the second-order terms in the gradients. The second term in Eq. (B6) cancels out as noted before. Then we have to retain only the zeroth order terms in the gradients (or $\boldsymbol{q}$ in the Fourier space) for $\langle\beta\mathcal{H}_1\rangle_0$ and we get

$$\langle\beta\mathcal{H}_1\rangle_0=v_0Nh_\phi(\boldsymbol{r}'). \tag{B7}$$

Finally, we obtain Eq. (40) by using Eqs. (A2), (B1), (B5), (B6), and (B7).

[1] For a review, see J.D. Gunton, M. San Miguel, and P.S. Sahni, in *Phase Transitions and Critical Phenomena*, edited by C. Domb and J. L. Lebowitz (Academic Press, New York, 1983), Vol. 8.

[2] For a review, see T. Hashimoto, Phase Transit. **12**, 47 (1988).

[3] P.G. de Gennes, J. Chem. Phys. **72**, 4756 (1980).

[4] P. Pincus, J. Chem. Phys. **75**, 1996 (1981).

[5] K. Binder, J. Chem. Phys. **79**, 6387 (1983).

[6] K. Kawasaki and K. Sekimoto, Physica A **148**, 361 (1988).

[7] T. Kawakatsu, Phys. Rev. E **56**, 3240 (1997).

[8] H. Tanaka, Phys. Rev. Lett. **71**, 3158 (1993).

[9] T. Taniguchi and A. Onuki, Phys. Rev. Lett. **77**, 4910 (1996).

[10] H. Tanaka and T. Araki, Phys. Rev. Lett. **78**, 4966 (1997).

[11] A. Onuki and T. Taniguchi, J. Chem. Phys. **106**, 5761 (1997).

[12] F. Brochard, J. Jouffroy, and P. Levinson, J. Phys. (Paris) **45**, 1125 (1984).

[13] C.L. Jackson and M.T. Shaw, Polymer **31**, 1070 (1990).

[14] C. Casagrande, P. Fabre, M.A. Guedeau, and M. Veyssie, Europhys. Lett. **3**, 73 (1987).

[15] C. Casagrande, M. Veyssie, and C.M. Knobler, Phys. Rev. Lett. **58**, 2079 (1987).

[16] A. Nakai, T. Shiwaku, H. Hasegawa, and T. Hashimoto, Macromolecules **19**, 3008 (1986); A. Nakai, T. Shiwaku, W. Wang, H. Hasegawa, and T. Hashimoto, Polymer **37**, 2259 (1996); Macromolecules **29**, 5990 (1996).

[17] T. Nagaya, H. Orihara, and Y. Ishibashi, J. Phys. Soc. Jpn. **58**, 3600 (1989).

[18] J.R. Dorgan, J. Chem. Phys. **98**, 9094 (1993).

[19] Y. Lansac, F. Fried, and P. Maissa, Liq. Cryst. **18**, 829 (1995).

[20] M. Doi and S.F. Edwards, *The Theory of Polymer Dynamics* (Oxford University Press, New York, 1986).

[21] T. Shimada, M. Doi, and K. Okano, J. Chem. Phys. **88**, 7181 (1988).

[22] A.J. Liu and G.H. Fredrickson, Macromolecules **29**, 8000 (1996).

[23] J. Fukuda (unpublished).

[24] J. Fukuda, Phys. Rev. E **58**, 6939 (1998).

[25] J. Fukuda, Eur. Phys. J. B (to be published).

[26] O. Kratky and G. Porod, Recl. Trav. Chim. Pays-Bas. **68**, 1106 (1949).

[27] N. Saitô, K. Takahashi, and Y. Yunoki, J. Phys. Soc. Jpn. **22**, 219 (1967).

[28] K.F. Freed, Adv. Chem. Phys. **22**, 1 (1972).

[29] R.A. Harris and J.E. Hearst, J. Chem. Phys. **44**, 2595 (1966); J.E. Hearst, R.A. Harris, and E. Beals, *ibid.* **45**, 3106 (1966).

[30] J.B. Lagowski, J. Noolandi, and B. Nickel, J. Chem. Phys. **95**, 1266 (1991).

[31] S.R. Zhao, C.P. Sun, and W.X. Zhang, J. Chem. Phys. **94**, 1572 (1997).

[32] P.G. de Gennes and J. Prost, *The Physics of Liquid Crystal*, 2nd ed. (Oxford University Press, New York, 1993).

[33] A.J. Liu and G.H. Fredrickson, Macromolecules **26**, 2817 (1993).

[34] A.M. Gupta and S.F. Edwards, J. Chem. Phys. **98**, 1588 (1993).

[35] A. Onuki and H. Nishimori, Phys. Rev. B **43**, 13 649 (1991).

[36] Y. Oono and S. Puri, Phys. Rev. A **38**, 434 (1988).